


Experimental conditions for obtaining halo p -wave dimers in quasi-one-dimensionFrancisco Fonta  and Kenneth M. O'Hara**Physics Department, The Pennsylvania State University, 104 Davey Lab, University Park, Pennsylvania 16802, USA*

(Received 13 May 2020; accepted 26 August 2020; published 19 October 2020)

We calculate the binding energy and closed-channel fraction of p -wave Feshbach molecules in quasi-one-dimension (quasi-1D) by examining the poles of the p -wave S matrix. We show that under the right experimental conditions, the quasi-1D p -wave molecule behaves like a halo dimer with a closed-channel fraction approaching 0 at resonance and a binding energy following the universal relation $E_b \sim 1/a_{1D}^2$, where a_{1D} is the 1D scattering length. We calculate these experimental conditions for both ${}^6\text{Li}$ and ${}^{40}\text{K}$ over a range of transverse confinements. We expect that in this halo dimer regime the three-body loss associated with the p -wave Feshbach resonance will be greatly suppressed, potentially allowing for a stable p -wave superfluid to be created. For an easy comparison between the three-dimensional and the quasi-1D cases, we provide the same pole analysis of the Feshbach molecules applied to the three-dimensional p -wave resonance and show that there is a qualitative difference between the two.

DOI: [10.1103/PhysRevA.102.043319](https://doi.org/10.1103/PhysRevA.102.043319)**I. INTRODUCTION**

Ultracold dilute Fermi gases near p -wave Feshbach resonances are of great interest due to the rich phases of matter associated with p -wave pairing. p -wave pairing is characterized by a more elaborate order parameter than s -wave pairing due to the different projections of the nonzero ($l = 1$) angular momentum. The distinct symmetries of the different angular momentum projections allow for sharp phase transitions between qualitatively different ground states as one tunes across the p -wave Feshbach resonance from the BEC side to the BCS side [1–5]. The s -wave BEC-BCS crossover, in contrast, features a smooth transition with no qualitative differences on either side of the resonance.

Experimentally, a dilute Fermi gas in three dimensions (3D) with controlled, resonant, p -wave interactions can in principle be realized with an optically trapped gas of fermionic alkali atoms (e.g., ${}^6\text{Li}$ or ${}^{40}\text{K}$) magnetically tuned near a p -wave Feshbach resonance. Such a gas would, at zero temperature, feature the sharp phase transitions mentioned above. Furthermore, by changing the trap configuration, p -wave pairing may be explored in reduced dimensions. In two dimensions, a $p_x + ip_y$ topological superfluid is expected [1,6–8], and in one dimension a fermionic Tonks Girardeau gas is predicted [9–14]. Furthermore, p -wave interactions on a one-dimensional lattice should reproduce the classic Kitaev chain model, which predicts the long sought after Majorana fermions [15]. However, despite significant experimental advancements in characterizing and manipulating p -wave Feshbach resonances [16–20], little progress has been made in stabilizing any of these novel phases. This is because unlike s -wave Feshbach resonances, p -wave Feshbach resonances

are accompanied by significant three-body and two-body loss [21–24].

While two-body loss can be mitigated in cases where the p -wave resonance occurs for atoms in their lowest hyperfine state, three-body loss is unavoidable. Three-body loss occurs when three particles are involved in a collision and subsequently two of the particles form a deeply bound dimer molecule, while the third particle allows for the conservation of energy and momentum in the exothermic reaction [28]. This loss mechanism can be enhanced by a Feshbach resonance through a process where a Feshbach molecule resonantly formed in the continuum collides with a third particle and subsequently decays to a more deeply bound molecular state. It is therefore important to understand the nature of Feshbach resonances and their underlying Feshbach molecules [29–31].

Resonant scattering occurs when a molecular bound state of the interacting particles is brought close to the continuum of free particle states (e.g., by application of a magnetic field). This connection between bound states and resonant interactions is seen most readily in the scattering S matrix, where the molecular bound states exist as poles of the S matrix [32]. For s -wave collisions near threshold and tuned close to resonance, the bound state associated with the Feshbach resonance is a halo dimer with a binding energy $E_b = \hbar^2/(ma^2)$, which only depends on the scattering length a . This is the so-called universal regime where, regardless of the specific atomic species, the only length scale governing the molecular state is the scattering length. The spatial wave function of this molecule is proportional to $\psi_l(r) \sim e^{-r/a}$, indicating that the molecular state becomes extremely delocalized as the scattering length diverges. This extremely delocalized molecule has virtually no wave function overlap with more deeply bound molecular states, thus effectively suppressing three-body loss. Conversely, due to the centrifugal barrier, p -wave resonances in 3D feature no such universal regime [20]. The underlying

*kohara@phys.psu.edu

p -wave Feshbach molecular state is well localized, with significant overlap with the more deeply bound molecular states, resulting in a very high likelihood of three-body loss.

In the coupled-channel picture, the Feshbach molecule is a dressed state

$$|\psi_{\text{mol}}\rangle = Z|\psi_{\text{closed}}\rangle + (1 - Z)|\psi_{\text{open}}\rangle, \quad (1)$$

which is a superposition of a free particle scattering state ψ_{open} and a bare molecular state ψ_{closed} . It is largely the closed-channel fraction $|Z|^2$ which leads to the three-body loss, as the closed-channel wave function has significant overlap with more deeply bound molecular states. In the two-body limit in 3D, the closed-channel fraction, $|Z|^2$, tends towards 0 as one approaches an s -wave Feshbach resonance. In contrast, as one approaches a p -wave Feshbach resonance, the closed-channel fraction, $|Z|^2$, remains significant and stays approximately constant. In the actual BEC-BCS crossover of an ultracold Fermi gas, many-body effects modify the Feshbach resonance [33–42]: in particular, even for s -wave resonances the closed-channel fraction has been shown to be nonzero, albeit very small and density dependent, at unitarity on through to the BCS side [37–42].

Recently, several studies have investigated ways to suppress three-body loss associated with p -wave resonances by considering scattering in lower dimensions [43–46]. Zhou and Cui, for example, have shown that in quasi-one-dimension (quasi-1D) the p -wave molecular wave function is significantly more delocalized than in 3D, suggesting that quasi-1D is a promising method for suppressing three-body loss [46]. Motivated by this work, our group as well as others has begun to study p -wave Fermi gases in quasi-1D. In a previous work we measured the three-body loss in lithium in quasi-1D [47]; while a significant suppression was observed, it is not clear that it is sufficient to stabilize the gas for an adequate time to reach equilibrium.

Here we expand on the results of Zhou and Cui [46]. By examining the poles of the S matrix we show that in quasi-1D a p -wave halo dimer exists in the two-body limit. We see that p -wave resonances in quasi-1D behave similarly to narrow s -wave resonances. We go on to characterize the 1D resonance for ^{40}K and ^6Li to determine the temperature, field stability, and transverse confinement needed to reach the halo dimer regime. Further, we determine the closed-channel fraction of the Feshbach-dressed molecule in quasi-1D and compare it to that in 3D. All of our calculations are in the two-body limit; while it is known that many-body effects will change the details of the resonance for an ultracold Fermi gas, it is our hope that the two-body physics presented here captures enough of the picture to serve as an effective guide for future experiments.

For the calculations in this paper related to ^6Li we consider the p -wave resonance between atoms in the $|F = \frac{1}{2}, m_f = +\frac{1}{2}\rangle$ state. For calculations related to ^{40}K we consider the p -wave resonance between atoms in the $|F = \frac{9}{2}, m_f = +\frac{7}{2}\rangle$ state with orbital angular momentum projected onto $m_l = 0$. The resonance parameters we use are reported in Table I.

TABLE I. p -wave scattering properties for ^6Li and ^{40}K [1,18,19,22,25–27].

	V_{bg} (units of a_0^3)	ΔB (G)	r_e (units of a_0^{-1})	B_{res} (G)	$\delta\mu_c$ ($\mu\text{K}/\text{G}$)
^6Li	-70×10^3	-40	-0.182	159.1	142
^{40}K	-10.49×10^5	-21.95	-0.0416	198.9	11.7

II. PHYSICAL SIGNIFICANCE OF POLES

Here we present a brief discussion relating the poles of the S matrix to bound states of the molecular potential [32]. Consider a partial-wave scattering state $\psi_l(k, r)$ that is the solution to a radial interacting potential. The asymptotic behavior of $\psi_l(k, r)$ is

$$\psi_l(k, r) \rightarrow \frac{i}{2r} [e^{-i(kr - l\frac{\pi}{2})} + S_l(k)e^{i(kr - l\frac{\pi}{2})}]. \quad (2)$$

For any such state, there exists a corresponding regular solution given by $\varphi_l(k, r) = F_l(k)\psi_l(k, r)$ behaving as

$$\varphi_l(k, r) \rightarrow \frac{i}{2r} [F_l(k)e^{-i(kr - l\frac{\pi}{2})} + F_l(-k)e^{i(kr - l\frac{\pi}{2})}], \quad (3)$$

where $F_l(k)$ is the Jost function and is related to the S matrix by $S_l(k) = F_l(-k)/F_l(k)$. It is clear that 0's of the Jost function are poles of the S matrix for which we consider solutions extended into the complex momentum plane. Consider a pole of the S matrix [corresponding to a 0 of $F_l(k)$] where the pole is purely positive imaginary, $k = \frac{i}{\hbar}\sqrt{m|E_b|}$. Then the regular solution, $\varphi_l(k, r) \sim e^{-|k|r}$, is a true bound-state solution of the Schrödinger equation with energy E_b . Conversely, a purely negative imaginary pole, $k = \frac{-i}{\hbar}\sqrt{m|E|}$, results in $\varphi_l(k, r) \sim e^{|k|r}$: a solution that cannot be normalized, which we call a virtual state. This state, while unphysical, still affects the underlying scattering process. Finally, a complex pole results in a state with complex energy, $E_{\text{pole}} = E_r - i\Gamma/2$. This corresponds to what we call a resonance, a quasistable state with energy E_r and lifetime $\tau = \frac{1}{\Gamma}$ [1,26]. It is this quasistable state embedded in the continuum which is thought to resonantly enhance three-body loss.

The poles of the scattering matrix thus give us direct access to the energy of the molecular bound state and the resonant state that is involved in three-body loss. Furthermore, we may use the dressed-state energy, E_b , to calculate the closed-channel amplitude as $Z = \partial(-E_b)/\partial(E_c)$, where E_c is the energy of the closed-channel molecular state [27,29,31].

III. POLE ANALYSIS OF P -WAVE RESONANCES IN 3D

To elucidate the problems leading to three-body loss near p -wave resonances we begin by examining the p -wave resonance in three dimensions. In all of the following we make the usual assumptions that the interatomic forces are short range and isotropic. We also assume that we are within the neighborhood of a p -wave resonance. The scattering process is then well described by an $l = 1$ partial-wave S matrix [1],

$$S = \frac{-\frac{1}{w} + \frac{1}{2}r_e k^2 + ik^3}{-\frac{1}{w} + \frac{1}{2}r_e k^2 - ik^3}, \quad (4)$$

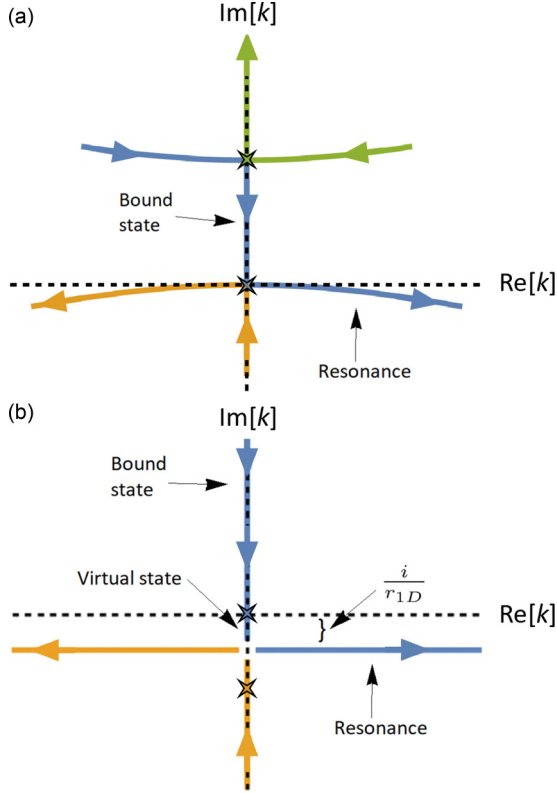


FIG. 1. Colored lines show the poles of the S matrix moving on the complex momentum plane in (a) 3D and (b) quasi-1D. Arrows show the direction in which the poles move as the magnetic field is tuned from the BEC side to the BCS side of the resonance. Stars show the locations of the poles in the complex k plane at $B = B_{\text{res}}$. (a) In 3D the pole corresponding to a bound state (blue) moves down the positive imaginary axis, becoming a resonance as soon as it crosses threshold. (b) In quasi-1D the bound-state pole moves down the positive imaginary axis and then continues along the negative imaginary axis as a “virtual state” until $k_{\text{pole}} = -\frac{i}{r_{1D}}$, and only then does it become a resonance.

where k is the relative momentum of the two atoms, w is the scattering volume, and r_e is the effective range, which for 3D p -wave resonances has units of inverse length. It is important to note that for the magnetically tuned Feshbach resonances we are interested in, the scattering volume w is a function of the magnetic field

$$w(B) = w_{bg} \left(1 - \frac{\Delta B}{B - B_0} \right), \quad (5)$$

where w_{bg} is the background scattering volume, B_0 is the bare resonance position, and ΔB is the resonance width.

The roots of $-\frac{1}{w} + r_e k^2/2 - ik^3$ with respect to k give the three poles of the S matrix. As we vary the scattering volume (by varying the magnetic field) the poles move on the complex plane [see Fig. 1(a)]. Importantly, one of these poles moves along the positive imaginary axis to cross the threshold and become a resonance. It is this pole corresponding to a true molecular bound state which then becomes a metastable state in the continuum that would potentially decay into a deeper molecular state upon collision with a third atom. The wave

number of this state is

$$k_{\text{pole}} = - \left(\frac{r_e}{6} + \frac{(i + \sqrt{3})r_e^2}{12(-r_e^3 - 108\alpha + 6\sqrt{6}\sqrt{\alpha(r_e^3 + 54\alpha)})^{\frac{1}{3}}} + \frac{i - \sqrt{3}}{12}(6\sqrt{6}\sqrt{\alpha(r_e^3 + 54\alpha)} - r_e^3 - 108\alpha)^{\frac{1}{3}} \right), \quad (6)$$

where α is $\frac{1}{w}$. As we approach resonance, the leading term in an expansion with respect to α gives $k_{\text{pole}} \rightarrow \sqrt{\frac{2}{wr_e}}$. Thus, as we approach resonance the bound-state energy scales as $E_{\text{pole}} = \hbar^2 k_{\text{pole}}^2/m \rightarrow 2\hbar^2/(mwr_e)$. There are two striking differences from the classic unitarity limited bound-state energy in s -wave resonances. First, the effective range is included in the energy, implying that the behavior is not universal across atomic species. Second, the binding energy scales as $1/w$, in contrast with the $1/a^2$ scaling of an s -wave Feshbach resonance in 3D. Because of this the p -wave binding energy approaches threshold as $(B - B_{\text{res}})$ instead of the typical s -wave behavior of $(B - B_{\text{res}})^2$.

To calculate the closed-channel amplitude, we note that $E_c = \delta\mu_c(B - B_0)$ is the closed-channel energy. We may then rewrite the scattering volume as

$$w = w_{bg} \left(1 - \frac{\delta\mu_c \Delta B}{E_c} \right). \quad (7)$$

Thus, we may rewrite $k_{\text{pole}}(w, r_e) \rightarrow k_{\text{pole}}(E_c, r_e)$ and consequently we may rewrite the binding energy E_b in terms of the closed-channel energy E_c . Simple differentiation, $Z = \partial(-E_b)/\partial(E_c)$, yields the closed-channel amplitude.

Figure 2 shows the closed-channel amplitude calculated for both ${}^6\text{Li}$ and ${}^{40}\text{K}$ close to their respective 3D p -wave resonances. Both closed-channel fractions remain approximately constant as they approach resonance. We calculate $Z = 0.8$ and $Z = 0.76$ for ${}^6\text{Li}$ and ${}^{40}\text{K}$, respectively, which are consistent with the measurements by Fuchs *et al.* [26] for ${}^6\text{Li}$ and Gaebler *et al.* [27,48] for ${}^{40}\text{K}$. The closed-channel fraction is thus large over the entire resonance for both atomic species. This is in stark contrast to s -wave resonances, where even for narrow resonances the closed-channel fraction approaches 0 as we approach resonance.

Figures 3(a) and 3(b) show the 3D p -wave scattering cross section as well as the Feshbach bound-state energy, E_b , for ${}^6\text{Li}$ and ${}^{40}\text{K}$, respectively. Note that both resonances are extremely narrow and that the bound state (solid line) tunes directly through the continuum to form a resonant state (dash-dotted line). The collision energy associated with the maximal scattering cross section directly follows the energy of the resonant state.

IV. ONE-DIMENSIONAL ANALYSIS

Now we extend the pole analysis to one dimension. In quasi-1D, Zhou and Cui found that you may write a new effective 1D S matrix [46],

$$S_{1D} = \frac{-\frac{1}{a_{1D}} + \frac{1}{2}r_{1D}k^2 + ik}{-\frac{1}{a_{1D}} + \frac{1}{2}r_{1D}k^2 - ik}, \quad (8)$$

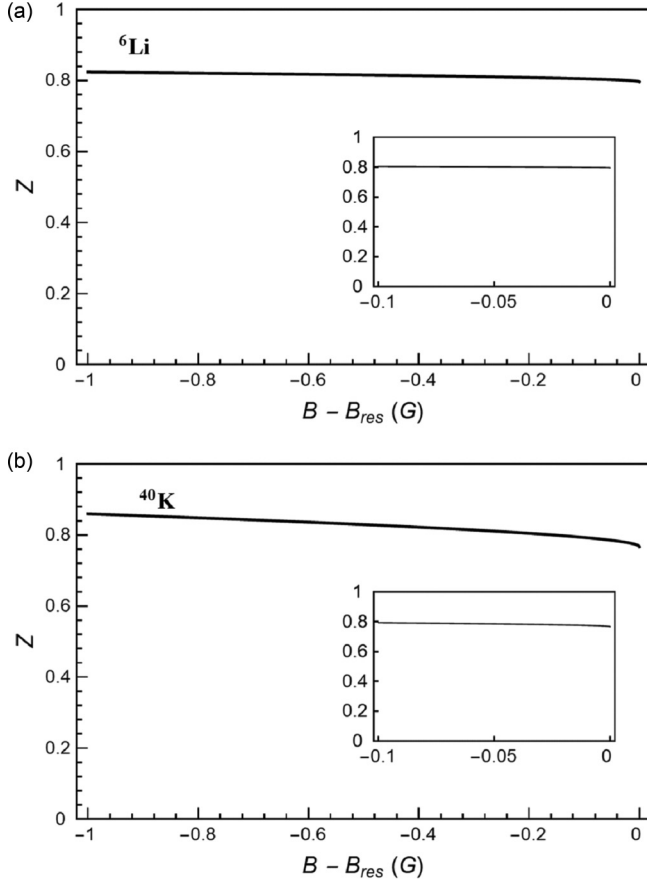


FIG. 2. Closed-channel amplitude in 3D for (a) ${}^6\text{Li}$ and (b) ${}^{40}\text{K}$. Inset: Closed-channel amplitude close to resonance.

where $a_{1\text{D}}$ is the effective 1D scattering length and $r_{1\text{D}}$ is the 1D effective range. The parameters are related to the 3D scattering volume and 3D effective range by

$$\frac{1}{a_{1\text{D}}} = \frac{a_{\perp}^2}{3} \left(\frac{1}{w} - \frac{1}{2} \frac{r_e}{a_{\perp}^2} \right) - \frac{1}{a_{\perp}^2} \zeta \left(-\frac{1}{2}, 1 \right), \quad (9)$$

$$r_{1\text{D}} = \frac{a_{\perp}^2 r_e}{3} - \frac{a_{\perp}}{\sqrt{2}} \zeta \left(\frac{1}{2}, 1 \right). \quad (10)$$

Here a_{\perp} is the transverse confinement length given by $a_{\perp} = \sqrt{\frac{\hbar}{m2\pi f_{\perp}}}$. For the remainder of the paper we quantify the confinement by the transverse trapping frequency f_{\perp} .

Figure 1 shows how the poles of the 1D S matrix move on the complex momentum plane. In contrast to the 3D case, there are only two poles. More importantly the pole corresponding to the true bound state crosses the threshold and then remains on the pure imaginary axis briefly before picking up a real part. In physical language the bound state becomes a virtual state and then becomes a resonance. It is this threshold behavior (bound state \rightarrow virtual state) that encapsulates the universal regime. Explicitly solving for the bound-state pole yields

$$k_{\text{pole1D}} = \frac{i - \sqrt{-1 + \frac{2r_{1\text{D}}}{a_{1\text{D}}}}}{r_{1\text{D}}}. \quad (11)$$

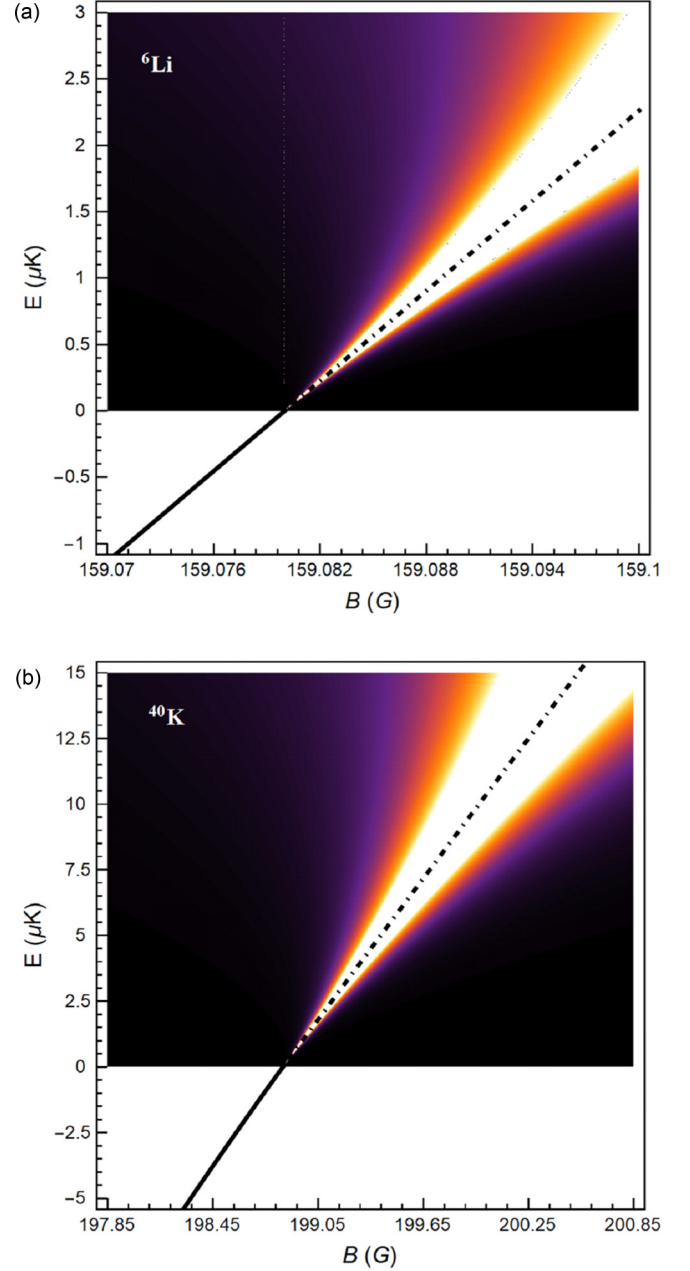


FIG. 3. Three-dimensional p -wave scattering cross section and bound-state energy for (a) ${}^6\text{Li}$ and (b) ${}^{40}\text{K}$. The bound-state energy (solid line) tunes linearly as a function of the magnetic field, directly becoming a resonance (dash-dotted line) at $B = B_{\text{res}}$, above which point the energy of this quasistable molecular state tunes linearly through the continuum.

Taking the limit as we approach resonance ($\frac{1}{a_{1\text{D}}} \rightarrow 0$), $k_{\text{pole1D}} \rightarrow \frac{1}{a_{1\text{D}}}$ reproduces the universal limit $E_{\text{pole}} \rightarrow \hbar^2/(ma_{1\text{D}}^2)$. This suggests that as we approach resonance the underlying molecular state is a halo dimer. To quantify this molecular state more fully, we calculate the closed-channel fraction.

We calculate the closed-channel amplitude the same way as in the 3D case; that is, owing to the poles we now have an expression for the 1D bound-state energy $E_{b,1\text{D}}$ in terms

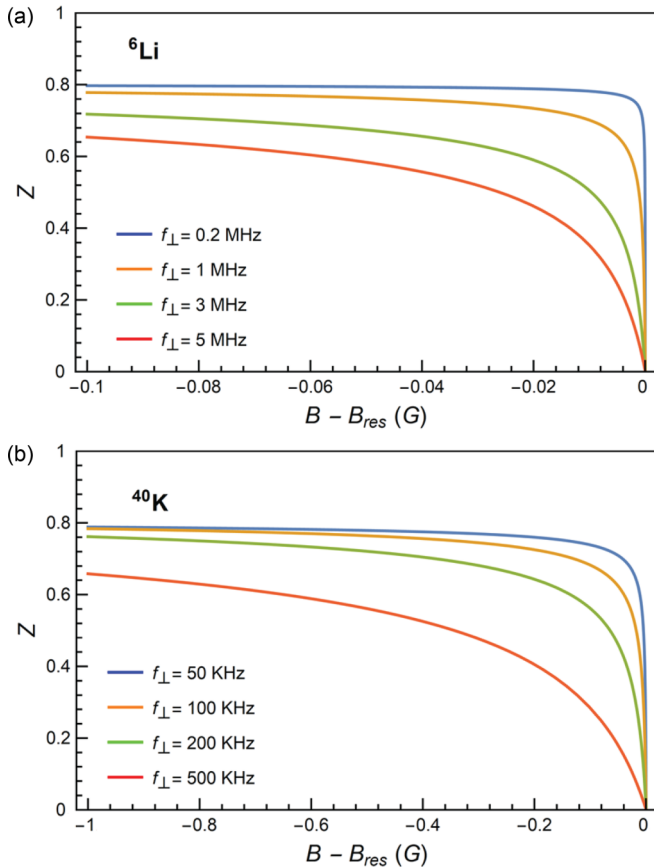


FIG. 4. Closed-channel amplitude in quasi-1D for (a) ${}^6\text{Li}$ and (b) ${}^{40}\text{K}$ for a variety of transverse confinements. The resonance becomes significantly more open channel dominated as the confinement increases.

of the closed-channel energy. Figure 4(a) [4(b)] shows the closed-channel amplitude calculated for ${}^6\text{Li}$ [${}^{40}\text{K}$] for a variety of transverse confinements. (Note that the confinement shifts the resonance position; we have shifted the origins to fit all the curves onto one plot.) The 1D p -wave closed-channel amplitude resembles the closed-channel amplitude of narrow s -wave resonances. Furthermore, as the confinement is increased the resonances become more and more open channel dominated. While for our two-body calculations the closed-channel amplitude goes to 0 on resonance, we expect many-body effects to keep Z nonzero throughout the resonance as they do in the s -wave case [37–42]. However, that Z goes to 0 in the two-body limit should imply that the closed-channel fraction becomes extremely small in the full many-body limit. It should be noted here that many-body effects also limit the universality of narrow s -wave resonances; when many-body effects are taken into account it has been shown that only resonances which are broad compared to the Fermi energy are truly universal [33–40,42]. However, a full many-body treatment of the problem is beyond the scope of this paper.

Next we consider the scattering cross section itself. Figure 5(a) [5(b)] shows the scattering cross section as well as the real part of the bound-state pole, $\text{Re}[E_{\text{pole}}]$, for ${}^6\text{Li}$ [${}^{40}\text{K}$]. For an experimentally realizable trap geometry which

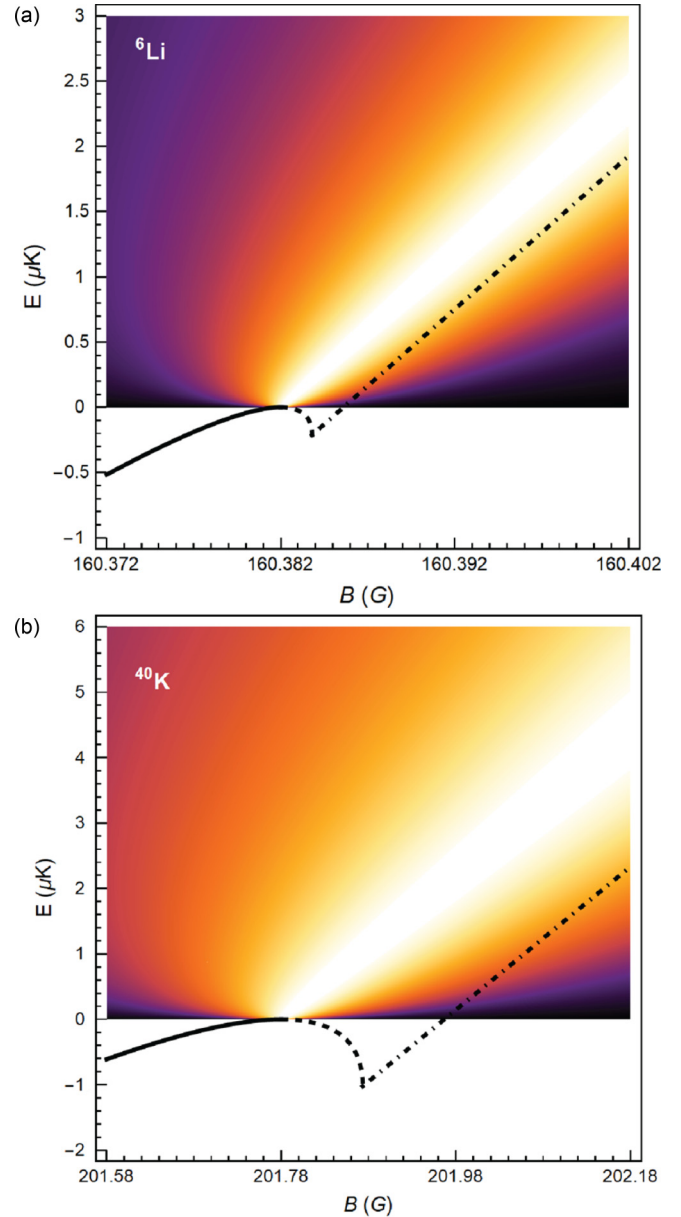


FIG. 5. Scattering cross section and bound-state energy in quasi-1D for (a) ${}^6\text{Li}$ and (b) ${}^{40}\text{K}$. We assumed a transverse confinement of 3 MHz (500 kHz) for ${}^6\text{Li}$ (${}^{40}\text{K}$). The energy of the bound state (solid line) merges with the continuum at B_{res} and then continues as a virtual state (dotted line) before eventually becoming a resonance (dash-dotted line).

can provide extremely tight confinement in two dimensions, we consider a square two-dimensional standing-wave lattice made from retroreflected 532-nm light with a depth of $200E_R$ (where E_R is the recoil energy for a 532-nm photon). This would correspond to a transverse confinement frequency of 3 MHz for ${}^6\text{Li}$ and 500 kHz for ${}^{40}\text{K}$. The solid line for energy represents the case where the pole is a true bound state; the dashed line, where it is a virtual state; and the dash-dotted line, where the pole is a resonance. Similarly to narrow s -wave resonances [1], we see that the energy of the two-body state varies quadratically with the magnetic field when the state is a true bound state and a virtual state near resonance. Once the

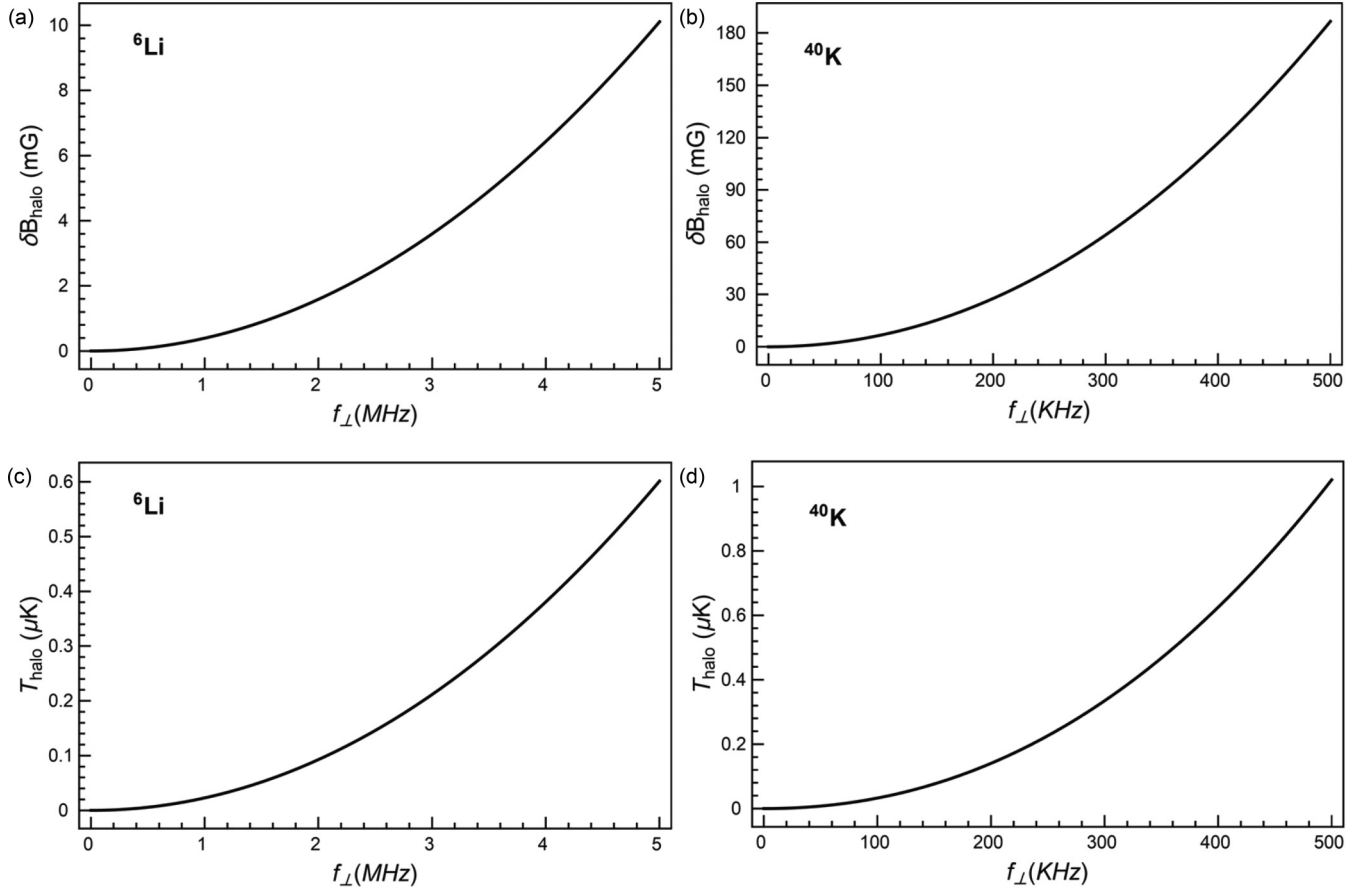


FIG. 6. [(a),(b)] Field stability and [(c),(d)] temperature required for achieving halo dimers as transverse confinement is increased. [(a),(c)] The conditions necessary for ${}^6\text{Li}$; [(b),(d)] the conditions necessary for ${}^{40}\text{K}$.

two-body state becomes a quasibound state it starts to vary linearly with the field.

We want to estimate the experimental conditions necessary to access the universal regime, $k_{\text{pole}} \sim \frac{1}{a_{1\text{D}}}$. It is clear from Fig. 5 that once the pole becomes a resonance there is a sharp change in behavior after which the energy of the pole scales linearly with the magnetic field. This transition occurs at $a_{1\text{D}}[f_{\perp}, B] = 2r_{1\text{D}}[f_{\perp}]$ and thus the unwanted resonance regime is avoided for $\frac{1}{a_{1\text{D}}} < \frac{1}{2r_{1\text{D}}}$. Next we want to ensure that k_{pole} is well approximated by a first-order expansion. Expanding k_{pole} to second order,

$$k_{\text{pole}} \rightarrow i \left(\frac{1}{a_{1\text{D}}} + \frac{r_{1\text{D}}}{2} \frac{1}{a_{1\text{D}}^2} \right), \quad (12)$$

we obtain the condition $\frac{1}{a_{1\text{D}}} \ll \frac{2}{r_{1\text{D}}}$. We take the requirement that no resonant states are formed to be sufficient as it is a factor of 4 more stringent than $\frac{1}{a_{1\text{D}}} < \frac{2}{r_{1\text{D}}}$; we believe that under these conditions the first-order approximation is adequately satisfied, however, there may still be some small deviation from the halo dimer form. To maintain this condition, very strict control of the magnetic field stability is necessary. For our suggested trap configuration, a field stability of $\delta B < 3.6$ mG for ${}^6\text{Li}$ and $\delta B < 187$ mG for ${}^{40}\text{K}$ is required. Furthermore, looking at the collisional energy where the scattering cross section is resonant, we may estimate the temperatures needed to reach this 1D p -wave halo dimer regime. For the

trap configuration in Fig. 5 this corresponds to a temperature of $T < 0.21 \mu\text{K}$ for ${}^6\text{Li}$ and $T < 1 \mu\text{K}$ for ${}^{40}\text{K}$. Note that the conditions for potassium are less stringent than those for lithium and thus it may be easier to suppress three-body loss in potassium. However, unlike lithium, potassium not only suffers from three-body loss but also suffers from two-body loss due to dipolar relaxation [21].

The confinement clearly plays a crucial role in achieving p -wave halo dimers. To identify requirements for future experiments aimed at realizing long-lived halo p -wave molecules, we have plotted in Fig. 6 the magnetic field stability and temperature necessary to access the universal regime for ${}^6\text{Li}$ and ${}^{40}\text{K}$ as a function of the transverse confinement. We use the conditions $a_{1\text{D}}[f_{\perp}, B_{\text{halo}}] < 2r_{1\text{D}}[f_{\perp}]$ and $T_{\text{halo}} < \hbar^2 / (k_B m r_{1\text{D}}[f_{\perp}]^2)$ to estimate the magnetic field stability and temperatures for which we expect halo dimers. Note that both δB_{halo} and T_{halo} increase very rapidly as the transverse confinement increases, making increasing the confinement a promising avenue for attaining the halo dimer region.

Thus far we have discussed the conditions for accessing the universal regime (achieving halo dimers) in quasi-1D p -wave Fermi gases. However, three-body loss may be suppressed even beyond the halo dimer regime. The energy of the pole in quasi-1D as a function of the magnetic field (see Fig. 5) shows that there is a sizable region in which there is no resonant state embedded in the continuum even though the scattering p -wave

cross section is still unitarity limited for small but nonzero values of k . This region is roughly twice as large as the halo dimer regime and consists of the cases where the pole is a true bound state, a virtual state, and a resonant state below threshold. Without a quasistable bound state embedded in the continuum, three-body loss would have to occur between three separate atoms rather than between one atom and one

quasistable molecule. Thus we expect three-body loss to be significantly suppressed within this entire region.

ACKNOWLEDGMENT

This work was supported by the National Science Foundation under Grant No. PHY-1607648.

-
- [1] V. Gurarie and L. Radzihovsky, *Ann. Phys.* **322**, 2 (2007).
- [2] V. Gurarie, L. Radzihovsky, and A. V. Andreev, *Phys. Rev. Lett.* **94**, 230403 (2005).
- [3] S. S. Botelho and C. A. R. Sá de Melo, *J. Low Temp. Phys.* **140**, 409 (2005).
- [4] C.-H. Cheng and S.-K. Yip, *Phys. Rev. Lett.* **95**, 070404 (2005).
- [5] M. Iskin and C. A. R. Sá de Melo, *Phys. Rev. Lett.* **96**, 040402 (2006).
- [6] N. Read and D. Green, *Phys. Rev. B* **61**, 10267 (2000).
- [7] A. K. Fedorov, V. I. Yudson, and G. V. Shlyapnikov, *Phys. Rev. A* **95**, 043615 (2017).
- [8] S. Tewari, S. Das Sarma, C. Nayak, C. Zhang, and P. Zoller, *Phys. Rev. Lett.* **98**, 010506 (2007).
- [9] M. D. Girardeau and E. M. Wright, *Phys. Rev. Lett.* **95**, 010406 (2005).
- [10] S. A. Bender, K. D. Erker, and B. E. Granger, *Phys. Rev. Lett.* **95**, 230404 (2005).
- [11] M. D. Girardeau and A. Minguzzi, *Phys. Rev. Lett.* **96**, 080404 (2006).
- [12] T. Cheon and T. Shigehara, *Phys. Rev. Lett.* **82**, 2536 (1999).
- [13] A. Imambekov, A. A. Lukyanov, L. I. Glazman, and V. Gritsev, *Phys. Rev. Lett.* **104**, 040402 (2010).
- [14] L. Pan, S. Chen, and X. Cui, *Phys. Rev. A* **98**, 011603(R) (2018).
- [15] A. Y. Kitaev, *Phys. Usp.* **44**, 131 (2001).
- [16] C. Luciuk, S. Trotzky, S. Smale, Z. Yu, S. Zhang, and J. H. Thywissen, *Nat. Phys.* **12**, 599 (2016).
- [17] C. Ticknor, C. A. Regal, D. S. Jin, and J. L. Bohn, *Phys. Rev. A* **69**, 042712 (2004).
- [18] C. H. Schunck, M. W. Zwierlein, C. A. Stan, S. M. F. Raupach, W. Ketterle, A. Simoni, E. Tiesinga, C. J. Williams, and P. S. Julienne, *Phys. Rev. A* **71**, 045601 (2005).
- [19] T. Nakasuji, J. Yoshida, and T. Mukaiyama, *Phys. Rev. A* **88**, 012710 (2013).
- [20] F. Chevy, E. G. M. van Kempen, T. Bourdel, J. Zhang, L. Khaykovich, M. Teichmann, L. Tarruell, S. J. J. M. F. Kokkelmans, and C. Salomon, *Phys. Rev. A* **71**, 062710 (2005).
- [21] C. A. Regal, C. Ticknor, J. L. Bohn, and D. S. Jin, *Phys. Rev. Lett.* **90**, 053201 (2003).
- [22] J. Zhang, E. G. M. van Kempen, T. Bourdel, L. Khaykovich, J. Cubizolles, F. Chevy, M. Teichmann, L. Tarruell, S. J. J. M. F. Kokkelmans, and C. Salomon, *Phys. Rev. A* **70**, 030702(R) (2004).
- [23] M. Waseem, J. Yoshida, T. Saito, and T. Mukaiyama, *Phys. Rev. A* **98**, 020702(R) (2018).
- [24] B. Deh, C. Marzok, C. Zimmermann, and P. W. Courteille, *Phys. Rev. A* **77**, 010701(R) (2008).
- [25] L. Austen, Ph.D. thesis, University College London (2012).
- [26] J. Fuchs, C. Ticknor, P. Dyke, G. Veeravalli, E. Kuhnle, W. Rowlands, P. Hannaford, and C. J. Vale, *Phys. Rev. A* **77**, 053616 (2008).
- [27] K. B. Gubbels and H. T. C. Stoof, *Phys. Rev. Lett.* **99**, 190406 (2007).
- [28] H. Suno, B. D. Esry, and C. H. Greene, *Phys. Rev. Lett.* **90**, 053202 (2003).
- [29] C. Chin, R. Grimm, P. Julienne, and E. Tiesinga, *Rev. Mod. Phys.* **82**, 1225 (2010).
- [30] H. Feshbach, *Ann. Phys.* **19**, 287 (1962).
- [31] T. Köhler, K. Góral, and P. S. Julienne, *Rev. Mod. Phys.* **78**, 1311 (2006).
- [32] J. R. Taylor, *Scattering Theory: The Quantum Theory on Non-relativistic Collisions* (John Wiley & Sons, New York, 1972).
- [33] R. Combescot, *Phys. Rev. Lett.* **91**, 120401 (2003).
- [34] G. M. Bruun, *Phys. Rev. A* **70**, 053602 (2004).
- [35] S. Simonucci, P. Pieri, and G. Strinati, *Europhys. Lett.* **69**, 713 (2005).
- [36] S. De Palo, M. L. Chiofalo, M. Holland, and S. Kokkelmans, *Phys. Lett. A* **327**, 490 (2004).
- [37] Q. Chen and K. Levin, *Phys. Rev. Lett.* **95**, 260406 (2005).
- [38] M. W. J. Romans and H. T. C. Stoof, *Phys. Rev. Lett.* **95**, 260407 (2005).
- [39] S. Zhang and A. J. Leggett, *Phys. Rev. A* **79**, 023601 (2009).
- [40] G. B. Partridge, K. E. Strecker, R. I. Kamar, M. W. Jack, and R. G. Hulet, *Phys. Rev. Lett.* **95**, 020404 (2005).
- [41] F. Werner, L. Tarruell, and Y. Castin, *Eur. Phys. J. B* **68**, 401 (2009).
- [42] X.-P. Liu, X.-C. Yao, H.-Z. Chen, X.-Q. Wang, Y.-X. Wang, Y.-A. Chen, Q. Chen, K. Levin, and J.-W. Pan, *arXiv:1903.12321* [cond-mat.quant-gas].
- [43] B. E. Granger and D. Blume, *Phys. Rev. Lett.* **92**, 133202 (2004).
- [44] S.-G. Peng, S. Tan, and K. Jiang, *Phys. Rev. Lett.* **112**, 250401 (2014).
- [45] L. Pricoupenko, *Phys. Rev. Lett.* **100**, 170404 (2008).
- [46] L. Zhou and X. Cui, *Phys. Rev. A* **96**, 030701(R) (2017).
- [47] A. S. Marcum, F. R. Fonta, A. Mawardi Ismail, and K. M. O'Hara, *arXiv:2007.15783* [physics.atom-ph] (2020).
- [48] J. P. Gaebler, J. T. Stewart, J. L. Bohn, and D. S. Jin, *Phys. Rev. Lett.* **98**, 200403 (2007).